Supporting Information

Rajapakse et al. 10.1073/pnas.1002025107

SI Text

SI Materials and Methods. All chemicals were purchased from Sigma Aldrich. Lumi4®-NHS was a kind gift from Lumiphore, Inc. Purified GFP-eDHFR was prepared as described previously (1). Dulbecco's modified eagle medium (DMEM), Dulbecco's phosphate buffered saline (PBS), Hank's buffered salt solution (HBSS), fetal bovine serum, Lipofectamine™ 2000 transfection reagent, buffers and reagents for pinocytosis/osmotic lysis (Influx™ reagent, cat. no. I-14402), and reagents for cell viability testing (LiveDead™ assay, cat. no. L3224) were purchased from Invitrogen, Inc. Streptolysin O (SLO) was obtained from MBL International, Inc. Low-resolution electrospray (ESI) mass spectra were obtained at the UIC Research Resources Center (RRC). UV-Vis absorption spectra were recorded using a Cary 3000 spectrophotometer (Varian, Inc.). Fluorescence emission spectra were recorded using a Fluoromax 3 fluorimeter (Horiba–Jobin Yvon, Inc.). Reversed-phase HPLC was performed using a Beckman System Gold instrument equipped with an analytical scale pump (model 128), a UV-Vis detector (model 168) and a C18 analytical column (GraceVydac, cat. no. 218TP54, 5 μm, 4.6 mm i.d. × 250 mm).

Synthesis of TMP-lumi4®. A derivative of trimethoprim substituted with an amine-terminated, 15-atom linker at the 4′ position (TMP-NH2) was prepared as previously described (1). TMP-NH2 (2 μmol, 1.0 eqiv.) was dissolved in 1.0 mL dry DMF and *ca.* 1 uL of diisopropyl ethylamine (*ca.* 5 μmol, 2.5 eqiv.) under nitrogen atmosphere. An N-hydroxy succinimidyl derivative of Lumi4® (Lumi4®-NHS) was dissolved in 0.5 mL DMF (2 μmol, 1.0 equiv) and added to the reactants. The solution was stirred at room temperature under nitrogen for 18 h. Product was purified by HPLC using 20 min linear gradient, from 5% to 35% solvent B (solvent A, 0.1 M triethylammonium acetate (pH 6.5) plus 5% CH_3CN; solvent B, CH_3CN). The fractions containing the desired compound were pooled, rotary evaporated to remove CH_3CN, and lyophilized to yield the desired compound. ESI-MS^+ ($C_{85}H_{115}N_{19}O_{20}$): m/z 1722.87 $[M + H]^+$.

Metal labeling. A stock solution of TMP-Lumi4 (300 μM in H_2O) was prepared. Concentration was estimated by measuring absorption at 339 nm and an extinction coefficient of 26,000 M^{-1} cm^{-1}. Aliquots were labeled with terbium as needed by combining with ~1.2 equiv. $TbCl_3$ in 1.5 mL centrifuge tubes, vortexing ~5 min, and resting at RT for *ca.* 30 min. Dilutions of the terbium-labeled compound into appropriate assay buffers could then be made for requisite spectroscopy or microscopy experiments.

Cell culture and transfection. NIH 3T3 and MDCKII cells were cultured in Dulbecco's Modified Eagle Media (DMEM, Invitrogen) supplemented with 10% FBS, 2 mM L-glutamine, 100 unit/mL penicillin and 100 mg/mL of streptomycin at 37 °C and 5% CO_2. NIH 3T3 and MDCK cells were passaged using 0.05% trypsin/0.03% EDTA solution (GIBCO) and 0.25% trypsin/0.03% EDTA solution, respectively.

Plasmids. Plasmid pLM1301 (expressing nucleus-localized CFP) described previously (2). Plasmid pLL1-NLS (expressing nucleus-localized eDHFR) was obtained from Active Motif, Inc. A plasmid expressing a C-terminal fusion of eDHFR to EGFP under constitutive control of the cytomegalovirus promoter was provided by Prof. V.W. Cornish. GFP-cldn1/tail was created by cloning amino acids 187–211 of human claudin-1 into pEGFP-C1 (Clontech). GFP-cldn1/$tail^{\Delta YV}$ was generated by point mutation to create a premature stop codon. ZO-1/PDZ1-eDHFR was created by inserting amino acids 19–113 of human ZO-1 (preceded by a start codon) into pLL-1NLS in frame with eDHFR. The integrity of all plasmids was verified by direct sequencing.

Cell transfection. NIH3T3 or MDCKII cells were seeded at 10^5 cells per well into a 6-well plate. After ~18 h incubation at 37 °C and 5% CO_2, adherent cells (~80% confluent) were transfected with 2 μg of the desired plasmid DNA using Lipofectamine2000™ transfection reagent (Invitrogen) according to manufacturer's instructions. Approximately 6 h after transfection, cells were trypsinized and reseeded at 14,000 cells/well into 8-well chambered slides and incubated at 37 °C and 5% CO_2 overnight.

Probe delivery via osmotic lysis of pinosomes. A 6 μL aliquot of TMP-Lumi4 (300 μM in H_2O) was combined with ~1.2 equivalents of $TbCl_3$ (in ~3 μL H_2O), vortexed for 5 min., and allowed to stand at room temperature for 30 min. This step effects chelation of terbium, rendering the probe luminescent. The metal-labeled TMP-Lumi4 solution (~9 μL) was combined with 27 μL of hypertonic growth medium (Influx™ reagent, Invitrogen, prepared according to manufacturer's instruction). NIH3T3 or MDCKII cells in a single well of an 8-well chambered slide were washed 1× with prewarmed (37º C) PBS and2× with prewarmed hypertonic solution, respectively. Then, prewarmed hypertonic solution containing TMP-Lumi4 was added, and the cells were incubated at 37 °C and 5% CO_2 for exactly 10 min. The cells were then quickly washed 2× with hypotonic solution (Influx™ reagent, Invitrogen, prepared according to manufacturer's instruction) and allowed to incubate in hypotonic solution for exactly 2 min. at room temperature to effect lysis of pinosomes. The cells were then washed 2× with PBS, immersed in complete DMEM and incubated for ~1 h at 37 °C and 5% CO_2 before imaging.

Probe delivery via streptolysin O (SLO)-mediated membrane permeabilization. SLO (1 mg/mL in PBS/50% glycerol, MBL International, Inc.) was diluted to a final concentration of 1000 ng/mL in 10 mM DTT/PBS and incubated at 37 °C for 2 h. The preactivated SLO was aliquoted and stored at −20 °C for later use. In a typical experiment, terbium-chelated TMP-Lumi4 was diluted to 15 μM in 100 μL Hank's buffered salt solution (HBSS). Preactivated SLO was added to a final concentration of 50 ng/mL (1:20 dilution of preactivated SLO stock solution). NIH3T3 or MDCKII cells in a single well of an 8-well chambered slide were washed 3× with prewarmed (37 °C) HBSS. Then, 150 μL of prewarmed TMP- Lumi4/SLO/HBSS solution was added, and the cells were incubated at 37 °C and 5% CO_2 for exactly 10 min. After incubation, 300 μL of DMEM containing 1.8 mM Ca^{2+} was added to the cells to effect resealing of membranes. The cells were incubated for at least 1 h at 37 °C and 5% CO_2 before washing 3× w/PBS and immersion in DMEM prior to imaging.

Cell viability assay. A standard assay for cell viability (Live-dead™ assay, Invitrogen, Inc., L3224) was used to assess the effects of SLO and osmotic lysis of pinosomes on MDCKII and NIH3T3 cells. Three separate experiments were performed for each cell type/treatment protocol, and the total number of living and dead

cells was summed. Greater than 93% of cells are alive 2 h after treatment ($n > 600$ for each condition, Table S1).

Live cell imaging. Microscopy of adherent live cells was performed using an epifluorescence microscope (Zeiss Axiovert 200) modified with the following components: (*i*) a fast-modulated UV LED emitting at 365 nm (UV-LED-365, Prizmatix, Ltd.); (*ii*) delay generator (DG645, Stanford Research Systems, Inc.); (*iii*) a gated image-intensified CCD camera (ICCD, mounted on the side-port of the microscope) and camera controller (Mega-10EX, Stanford Photonics, Inc.); and (*iv*) a computer running Piper Control software (v2.4.05, Stanford Photonics, Inc.). A 100 W mercury arc lamp was available for continuous wave fluorescence excitation, and a conventional CCD (Zeiss Axiocam MRM) was mounted on the front port of the microscope. Filter cubes containing the appropriate excitation and emission filters and dichroics allowed for wavelength selection. Samples were imaged with a 63X/1.25 N.A. EC Plan Neofluar oil-immersion objective (Carl Zeiss, Inc.) For continuous-wave fluorescence and bright field images, the ICCD was set to "Live" mode, with automatic gain level and acquisition time.

The UV LED excitation source provides a collimated output that we measured to equal ~50 mW at the exit window. The LED circuitry allows for continuous wave emission or external TTL modulation with submicrosecond rise/fall times. The excitation intensity could be varied, however, we held the intensity constant at a measured value of 1.6 mW at the objective back aperture. Using the method of Grünwald, et al. (3) we estimated the illumination intensity to equal ~0.6 W/cm^2 at the image plane when using the Zeiss EC Plan Neofluar 63× 1.25 N.A. objective.

For time-resolved microscopy with pulsed, near-UV excitation, image acquisition was initiated by a start signal (TTL) from the computer to the delay generator. Separate outputs (TTL) routed from the delay generator to the UV LED and the ICCD (via the camera controller) relayed a preprogrammed "burst" sequence to trigger the LED and the intensifier a user-defined number of times. For each acquisition, the signal from multiple excitation/emission events was accumulated on the ICCD sensor and read out to the image capture card of the computer at the end of the camera frame. The UV LED pulse width and pulse period, the intensifier delay time and on-time, the camera frame length (66.67 ms–2 s) and the intensifier gain voltage could be varied independently.

The source/camera timing parameters were the same for all of the time-resolved images and data presented here: excitation pulse width = 1500 μs, pulse period = 3000 μs, delay time = 10 μs, intensifier on-time = 1390 μs. The sensitivity of the time-resolved microscope is partly dependent on the number of excitation/detection events integrated on the CCD during a single camera frame and on the intensifier gain voltage. The signal-to-noise ratio, and thus the precision with which time-resolved data can be acquired is improved by summing multiple frames to generate a single image (at the expense of longer image acquisition times). Each frame summed effectively increases the bit depth of the resulting image by a factor of 1024 (i.e., 1 frame yields bit depth equal to 1024, 2 frames, 2048, etc.). A feature of the camera control software was enabled that removes large variations in signal resulting from ion-feedback noise of the intensifier. Table S2 lists the number of excitation/detection events, frame length, number of frames, total acquisition time and intensifier gain voltage used to acquire all time-resolved images and/or datasets reported in the paper and in *SI Text*.

Image processing and data analysis. Images (tagged image file format, .TIF) were captured with Piper control software (v2.4.05, Stanford Photonics, Inc.). and rendered using NIH Image J (v1.34). Micrographs showing LRET images and their associated controls were presented with identical contrast levels. Table S2 provides the image processing parameters applied to each time-resolved image in the paper, including pixel dimensions, pixel (bit) depth and contrast level (minimum and maximum gray values).

For quantitative analysis of time-resolved microscope images, the emission signal intensity was calculated according to the equation: $S = (\mu_{signal}\text{-}\mu_{bckg})$, where, μ_{signal} is equal to the mean pixel gray value in a region of interest (ROI) corresponding to the area of a cell, and μ_{bckg} is equal to the mean pixel gray value in a nearby ROI of equivalent area, (Fig. S3). The donor-normalized LRET signal (LRETN) was defined as S_{520}/S_{540}, where S_{520} was the net LRET signal measured through a narrow-pass filter that collected only a portion of the GFP emission ($\lambda_{em} = 520 \pm 10$ nm) and S_{540} represented a signal that comprised sensitized GFP emission and directly excited terbium emission ($\lambda_{em} = 540 \pm 10$ nm). Cells were selected for analysis that exhibited both GFP expression and loading of TMP-Lumi4 as determined by examining corresponding continuous wave fluorescence images ($\lambda_{ex} = 480 \pm 20$ nm, $\lambda_{em} = 535 \pm 25$ nm) and time-resolved images of terbium emission ($\lambda_{ex} = 365$ nm, $\lambda_{em} = 540 \pm 10$ nm). Intramolecular LRETN was calculated for cells expressing GFP-eDHFR. Intermolecular LRETN was calculated for cells expressing interacting proteins (ZO-1/PDZ1-eDHFR and GFP-cldn1/tail) and for cells expressing putatively noninteracting proteins (ZO-1/PDZ1-eDHFR and GFP-cldn1/tail$^{\Delta YV}$). The mean, standard deviation and range of LRETN was determined for each sample. *P*-value was determined from a two-tailed, two-sample, unequal variance t-test of the interacting and putatively noninteracting, intermolecular LRETN samples (Table S3).

Luminescent lifetime estimation and calculation of in vitro LRET energy transfer efficiency. Stock solutions of TMP-Lumi4 and Lumi4®-Tb were chelated with terbium, diluted to ~20 nM in assay buffer (50 mM K_2HPO_4, KH_2PO_4, 18 mM β-mercaptoethanol, 10 μM NADPH, pH 7.2). Fluorescence intensity was measured using a time-resolved fluorescence plate reader (Perkin Elmer, Victor 3V) with 340 nm excitation (60 nm bandpass) and 545 nm emission (10 nm bandpass). Intensity values (500 μs integration) were measured at different time delays from 100 μs to 2500 μs (100 μs increments). Plots of intensity vs. delay time were fit to a single exponential with KaleidaGraph v4.0 (Fig. S1), and lifetime was estimated from the equation: $I(t) = I_0 \exp(-t/\tau)$ (4). The measurements were repeated 3× to yield mean estimated lifetimes: Lumi4®-Tb, 2.35 ± 0.05 ms (mean ± s.e.m.); TMP-Lumi4, 2.28 ± 0.07 ms (mean ± s.e.m.).

To measure the lifetime of terbium-sensitized GFP emission, TMP-Lumi4 and GFP-eDHFR were diluted to 20 nM and 100 nM, respectively in assay buffer (50 mM K_2HPO_4, KH_2PO_4, 18 mM β-mercaptoethanol, 10 μM NADPH, pH 7.2). Lifetime was determined by single exponential fit to plots of intensity (340 nm exciation, 520 nm emission) vs. delay time (Fig. S1). Three repetitions yielded the mean estimated lifetime of terbium-sensitized GFP emission: 0.78 ± 0.04 ms (mean± s.e.m.).

The efficiency of energy transfer from terbium-to-GFP in the TMP-Lumi4/GFP-eDHFR complex was calculated from the equation, $E = 1 - \tau_A/\tau_D$, where τ_A is the lifetime of sensitized GFP emission and τ_D is the lifetime of TMP-Lumi4 (5). From lifetime data, a value of 0.67 was calculated.

1. Rajapakse HE, Reddy DR, Mohandessi S, Butlin NG, Miller LW (2009) Luminescent terbium protein labels for time-resolved microscopy and screening. *Angew Chem Int Ed Engl* 48(27):4990–4992.

2. Miller LW, Cai Y, Sheetz MP, Cornish VW (2005) In vivo protein labeling with trimethoprim conjugates: A flexible chemical tag. *Nat Methods* 2(4):255–257.

3. Grunwald D, Shenoy SM, Burke S, Singer RH (2008) Calibrating excitation light fluxes for quantitative light microscopy in cell biology. *Nat Protoc* 3(11):1809–1814.
4. Lakowicz JR (2006) Principles of fluorescence spectroscopy, 3rd ed. (Springer, New York), p. 99.
5. Selvin PR, Hearst JE (1994) Luminescence energy transfer using a terbium chelate: Improvements on fluorescence energy transfer. *Proc Natl Acad Sci USA* 91(21): 10024–10028.

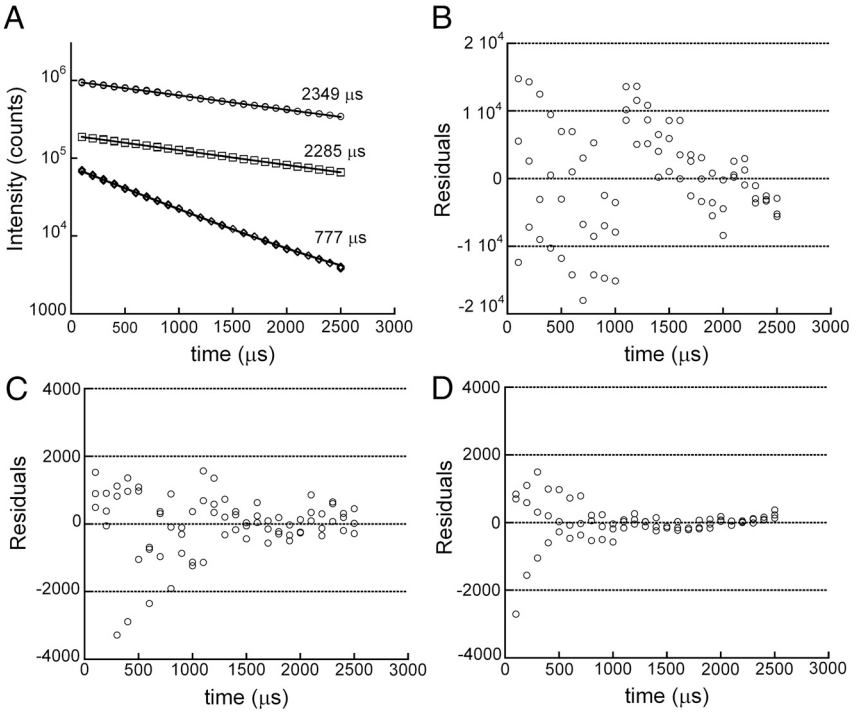

Fig. S1. Results of emission lifetime analyses. (*A*) Representative intensity vs. time plots of Lumi4-Tb (circles), TMP-Lumi4 (squares) and terbium-sensitized GFP emission from a TMP-Lumi4/GFP-eDHFR complex (diamonds), measured as described in *SI Materials and Methods*. For Lumi4-Tb and TMP-Lumi4, the solid line is a single exponential (2 parameter) fit to the data, $I(t) = I_0 \exp(-t/\tau)$. For sensitized GFP emission, the data were fit to a single exponential decay with an offset (3 parameter), $I(t) = A + I_0 \exp(-t/\tau)$. The calculated lifetime is shown adjacent to the plotted curves, and three repetitions of the experiment yielded values that agreed within <4 percent. The 3 parameter fit for the sensitized emission curve yielded an offset value <2% of the amplitude in all cases. The r^2 residuals were greater than 0.99 in call cases, and residual plots showed no structure. (*B*)–(*D*) Residual plots for Lumi4-Tb, TMP-Lumi4, and sensitized GFP emission, respectively.

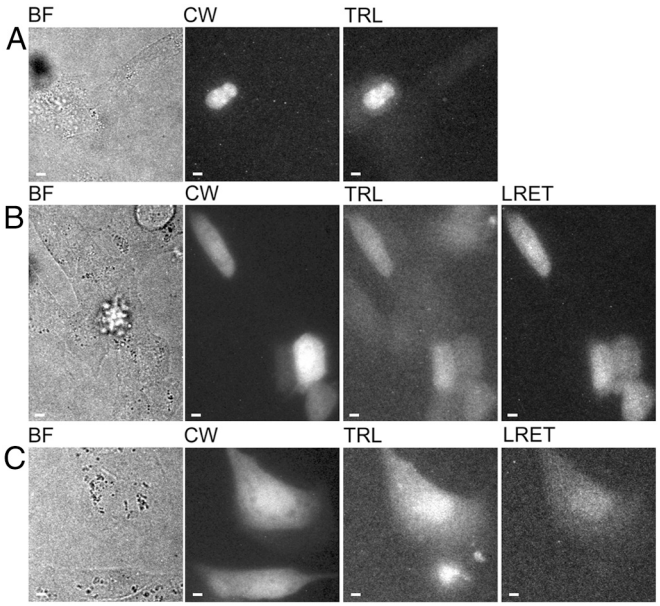

Fig. S2. Additional images showing that both SLO-mediated membrane permeabilization and osmotic lysis of pinocytic vesicles can be used to deliver TMP-Lumi4 to the cytoplasm of at least two cell types: NIH3T3 fibroblasts and MDCKII epithelial cells. Upon delivery into cells, TMP-Lumi4 binds specifically to eDHFR fusion proteins, and the specific binding can be visualized by time-resolved luminescence microscopy. Micrographs: BF, bright field; CW, continuous-wave fluorescence ($\lambda_{ex} = 480 \pm 20$ nm, $\lambda_{em} = 535 \pm 25$ nm); TRL, time-resolved fluorescence ($\lambda_{ex} = 365$ nm, $\lambda_{em} > 400$ nm, gate delay $= 10$ μs); LRET, time-resolved LRET ($\lambda_{ex} = 365$ nm, $\lambda_{em} = 520 \pm 10$ nm, gate delay $= 10$ μs). Scale bars, 10 μm. (*A*) NIH3T3 fibroblast cells transiently cotransfected with DNA encoding nucleus-localized CFP and nucleus-localized eDHFR were incubated with TMP-Lumi4 (15 μM) and streptolysin O (SLO, 50 ng/mL) for 10 min. Time-resolved detection of broadband (>400 nm) terbium emission reveals localization of TMP-Lumi4 in nucleus of transfected cell (corresponding to continuous wave fluorescence image of CFP emission). (*B*) NIH3T3 fibroblast cells transiently transfected with DNA encoding GFP-eDHFR. Cells were incubated in hypertonic medium containing TMP-Lumi4 (50 μM) for 10 min. to allow pinocytosis and subsequently exposed to hypotonic medium to effect lysis of pinocytic vesicles and release of probe into the cytoplasm. Time-resolved detection of broadband emission (>400 nm) reveals terbium luminescence in TMP-Lumi4-loaded cells. Luminescence resonance energy transfer (LRET) is seen only in transfected cells (indicated in continuous wave fluorescence image) coincidentally loaded with TMP-Lumi4 when visualized in time-resolved mode through a narrow-pass filter (520 ± 10 nm), indicating specific labeling of the GFP-eDHFR fusion protein. (*C*) MDCKII cells coexpressing ZO-1/PDZ1-eDHFR and GFP-cldn1/tail were incubated with TMP-Lumi4 (15 μM) and streptolysin O (SLO, 50 ng/mL) for 10 min. Terbium-to-GFP LRET is seen only in transfected cells loaded with TMP-Lumi4.

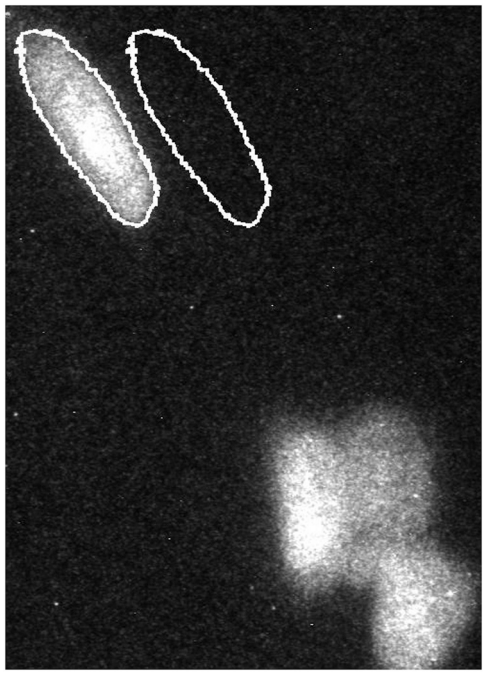

Fig. S3. Representative regions of interest (ROIs) used to calculate LRET signal levels as described in *SI Materials and Methods*.

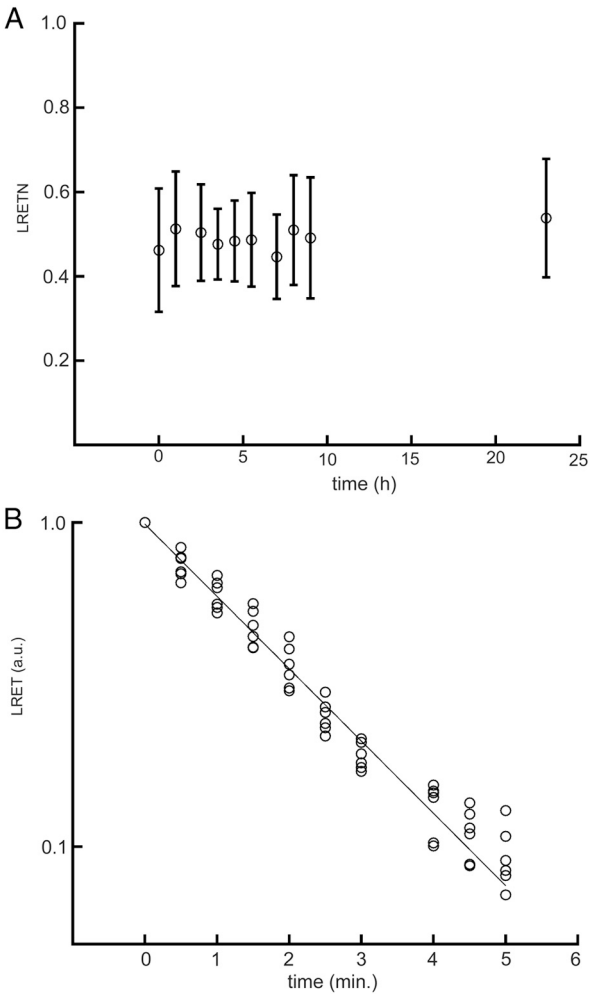

Fig. S4. TMP-Lumi4 is stably luminescent in cells and resistant to photobleaching. (*A*) Plot of mean ± s.d., donor-normalized LRET signal (LRETN) vs. time obtained from time-resolved images of MDCKII cells expressing GFP-eDHFR and pinocytically loaded with TMP-Lumi4. LRETN equals the 520 nm/540 nm emission signal ratio, where emission signal was measured as the background-subtracted mean gray value for a single cell in an image. More than 10 cells were used to calculate mean LRETN at each time point. (*B*) Semilog plot of LRET signal intensity (normalized to initial value at $t = 0$) vs. accumulated irradiation time for MDCKII cells expressing GFP-eDHFR and pinocytically loaded with TMP-Lumi4. A field of view was exposed to continuous wave LED excitation at the standard illumination intensity (~0.6 W/cm^2), imaged at successive timepoints ($\lambda_{ex} = 365$ nm, $\lambda_{em} = 520 \pm 10$ nm, gate delay = 10 μs), and the background-subtracted mean gray value determined for each cell exhibiting LRET in the field. The solid line is a single exponential (2 parameter) fit to the data, $y = a^* \exp(-t/\tau)$. For the data shown, $\tau = 1.95 \pm 0.05$ min and $r^2 = 0.98$. The experiment was performed 3 times, and τ ranged from 1.9–2.1 min. with $r^2 > 0.97$ in all cases ($n > 5$ cells for each experiment). Specific imaging parameters are provided in Table S2.

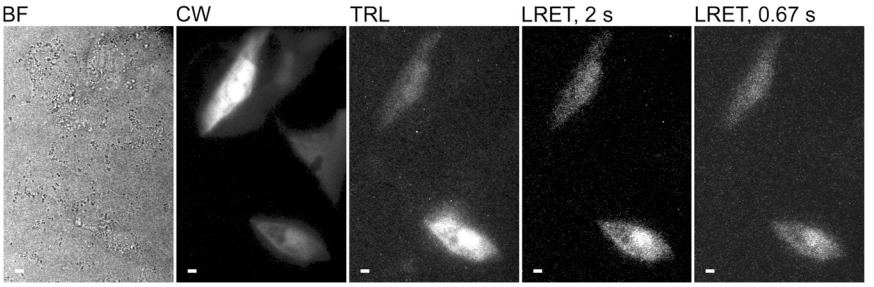

Fig. S5. Rapid detection of intermolecular LRET between TMP-Lumi4-labeled ZO-1/PDZ1-eDHFR and GFP-cldn1/tail. MDCK cells coexpressing ZO-1/PDZ1-eDHFR and GFP-cldn1/tail. Cells were loaded by pinocytosis (10 min) of culture medium containing TMP-Lumi4 (60 μM) followed by osmotic lysis of pinosomes. Micrographs: BF, bright field; CW, continuous wave fluorescence ($\lambda_{ex} = 480 \pm 20$ nm, $\lambda_{em} = 535 \pm 25$ nm); TRL, time-resolved fluorescence ($\lambda_{ex} = 365$ nm, $\lambda_{em} > 400$ nm, gate delay = 10 μs); LRET, time-resolved images ($\lambda_{ex} = 365$ nm, $\lambda_{em} = 520 \pm 10$ nm, gate delay = 10 μs) acquired in a single frame of indicated length. Both LRET images were adjusted to identical contrast levels (50/300 min/max). Scale bars, 10 μm.

Table S1. Summary of Live-Dead Assay™ (Invitrogen, L3224) assessment of the effects of SLO and osmotic lysis of pinosomes on MDCKII and NIH3T3 cells, 2 h posttreatment

	MDCK		NIH3T3	
	SLO	Pinocytosis	SLO	Pinocytosis
Total	691	1521	927	1056
Live (%)	657 (95.08)	1423 (93.56)	878 (94.71)	992 (93.94)
Dead (%)	34 (4.92)	98 (6.44)	49 (5.29)	64 (6.06)

Table S2. Summary of detection and image processing parameters for all time-resolved images and data presented in the paper

Image or data	λ_{em} (nm)	Excitation events	Frame length (ms)	Frames	Acquisition time (ms)	Intensifier gain (V)	Pixel dimensions	Pixel depth	Contrast (min / max)*
Fig. 3*A*, TRL	>400	220	666	1	666	778	500 × 500	1024	150/1000
Fig. 3*A*, TRL + TMP	>400	220	666	1	666	778	500 × 500	1024	150/1000
Fig. 3*B*, TRL	>400	110	333	4	1333	833	500 × 700	4096	316/4092
Fig. 3*B*, LRET	510–530	330	1000	4	4000	833	500 × 700	4096	150/1000
Fig. 4*A*, TRL	>400	110	333	4	1066	778	750 × 750	4096	510/2952
Fig. 4*A*, LRET	510–530	660	2000	4	8000	778	750 × 750	4096	150/1000
Fig. 4*A*, LRET + TMP (2 min)	510–530	660	2000	4	8000	778	750 × 750	4096	150/1000
Fig. 4*A*, LRET + TMP (20 min)	510–530	660	2000	4	8000	778	750 × 750	4096	150/1000
Fig. 4*B*, TRL	>400	220	666	4	2667	778	750 × 750	4096	722/4078
Fig. 4*B*, LRET	510–530	660	2000	4	8000	778	750 × 750	4096	150/1000
Table S3	†	660	2000	4	8000	889	N/A	4096	N/A
Fig. S2*A*, TRL	>400	220	666	1	666	778	500 × 500	1024	93/1020
Fig. S2*B*, TRL	>400	110	333	4	1333	778	500 × 700	4096	396/4092
Fig. S2*B*, LRET	510–530	660	2000	4	8000	778	500 × 700	4096	130/2223
Fig. S2*C*, TRL	>400	110	333	8	1333	889	500 × 500	8192	907/4154
Fig. S2*C*, LRET	510–530	660	2000	4	8000	922	500 × 500	4096	150/1500
Fig. S4*A*	†	330	1000	4	4000	833	N/A	4096	N/A
Fig. S4*B*	510–530	660	2000	4	8000	889	N/A	4096	N/A
Fig. S5, TRL	>400	44	133	1	133	778	600 × 900	1024	61/1019
Fig. S5, LRET, (2 s)	510–530	330	1000	2	2000	778	600 × 900	2048	50/300
Fig. S5, LRET, (0.67 s)	510–530	110	333	2	666	778	600 × 900	2048	50/300

*Contrast indicates minimum and maximum gray level values used to represent respective images.
†For quantitative analysis of donor-normalized LRET signals (presented in Table S3 and Fig. S4*A*), 2 images were acquired using the indicated source/camera parameters: acceptor emission (510–530 nm) and donor emission + acceptor emission (530–550 nm).

Table S3. Summary of donor-normalized LRET (LRETN) data* for cells expressing interacting (ZO-1/PDZ1-eDHFR and GFP-cldn1/tail) and noninteracting (ZO-1/PDZ1-eDHFR and GFP-cldn1/tail$^{\Delta YV}$) proteins

	ZO-1/PDZ1-eDHFR GFP-cldn1/tail	ZO-1/PDZ1-eDHFR GFP-cldn1/tail$^{\Delta YV}$
No. cells	11	9
Mean	0.38	0.06
S.d.	0.10	0.04
Range	0.17–0.50	0.02–0.11
t-test *p* value = 3.4×10^{-7}†		

*Calculated as described in the main article and in *SI Materials and Methods* from time-resolved images acquired using parameters listed in Table S2.
†Calculated from a two-tailed, two-sample, unequal variance *t*-test of the interacting and putatively noninteracting LRETN samples.